

MULTI-FRAGMENT PRODUCTION IN THE $^{32}\text{S}+^{58,64}\text{Ni}$ REACTIONS
AT 11 A MeV

F. GRAMEGNA^a, U. ABBONDANNO^b, A. BONASERA^c, M. BRUNO^d, G. CASINI^e,
S. CAVALLARO^{c,f}, M. CHIARI^e, M. D'AGOSTINO^d, A. LANCHAIS^d,
G. V. MARGAGLIOTTI^b, P. F. MASTINU^a, P. M. MILAZZO^b, A. MORONI^g, A.
NANNINI^e, A. ORDINE^h, R. A. RICCI^a, F. TONETTO^b, L. TRAVAGLINI^a,
G. VANNINI^d and L. VANNUCCI^a

^a*Istituto Nazionale di Fisica Nucleare, Laboratori Nazionali di Legnaro, Italy*

^b*Istituto Nazionale di Fisica Nucleare, Sezione di Trieste and Dipartimento di Fisica
dell'Università, Trieste, Italy*

^c*Istituto Nazionale di Fisica Nucleare, Laboratori Nazionali del Sud, Catania, Italy*

^d*Istituto Nazionale di Fisica Nucleare, Sezione di Bologna and Dipartimento di Fisica
dell'Università, Bologna, Italy*

^e*Istituto Nazionale di Fisica Nucleare, Sezione di Firenze, Italy*

^f*Dipartimento di Fisica dell'Università, Catania, Italy*

^g*Istituto Nazionale di Fisica Nucleare, Sezione di Milano, Italy*

^h*Istituto Nazionale di Fisica Nucleare, Sezione di Napoli, Italy*

Paper devoted to honour the memory of Professor Nikola Cindro

Received 27 June 2002; revised manuscript received 26 February 2003

Accepted 10 March 2003 Online 20 September 2003

The characteristic features of the $^{32}\text{S}+^{58,64}\text{Ni}$ reaction at 11 A MeV have been investigated to evidence the possible rise of multi-fragmentation processes at low excitation energies. The importance of such phenomena consists in the fact that they could represent the signature of a nuclear phase transition from a liquid to a gas region. Evidence of multi-fragment production is displayed by the present data; even if the yield of such events is compatible with the predictions of statistical models, the partition of the mass of the decaying system cannot be easily reproduced. Some preliminary indications of isospin effects are suggested by looking at the differences between the two reacting systems.

PACS numbers: 25.70 Pq

UDC 539.172

Keywords: heavy ions, multi-fragmentation, nuclear phase transition

1. Introduction

The phenomena characterizing the low energy domain in heavy-ion nuclear studies (below ~ 10 A MeV) are almost completely understood. They are usually classified according to the impact parameter b or the orbital angular momentum L . One can travel quite easily as a function of decreasing b , from elastic scattering, through few nucleon transfer and deep inelastic collisions to compound nucleus formation, looking at the amount of energy and angular momentum which can be transferred from the relative motion to the intrinsic degrees of freedom. In this energy range, the composite system, formed in central collisions ($b \leq b_{\text{crit}}$), can generally undergo statistical de-excitation through evaporation of light particles (mainly neutrons, protons or α -particles) and γ -rays. The compound system can also fission more or less symmetrically, depending on the particular shape of the potential energy surface, which strongly depends on the angular momentum (the fission barrier is known to vanish for particular values of angular momentum) [1].

At higher incident energies, the scenario evolves towards phenomena that are more complex. The energies available to the systems increase and the reaction time becomes shorter and shorter. To describe this complex reaction scenario one has to characterize the reaction system by disentangling and selecting emission sources and by detecting and identifying literally all reaction products in as much details as practicable, including low detection thresholds and good energy, charge and mass resolution.

Some of these processes, going from low to intermediate energies, seem to be quite important: they deal with the multifragmentation, i.e. the presence in the exit channel of multiplicities higher than 2 with fragments of charge $Z > 2$ (intermediate mass fragments, IMF). Multi-fragment emission, being considered as a signature of the change in the behaviour of the nuclear matter in extreme conditions of temperature and density, has been one of the fashioning themes of research in the intermediate energy regime in the last decade. For many years, the nature of the mechanisms responsible for the production of IMFs has been discussed: these fragments could come from a sequential statistical decay, like subsequent fission processes characterized by quite long emission times between one step and the following, or could be emitted in a fast, almost prompt way (multi-fragmentation), or eventually could be dynamically driven (no complete equilibrium reached in the system).

All these possibilities are present at higher energies and must be disentangled through deep and complete studies of the most exclusive observable, capable to extract the peculiar characteristics of the different reaction mechanisms. A variety of different models, from statistical sequential models (GEMINI) [2] to statistical multi-fragmentation models (SMM) [3, 4] and to dynamical models (classical molecular dynamics (CMD) [5, 6] and quantum molecular dynamics (QMD) [7]) could often describe the inclusive distributions resulting from experiments with multi-IMF production. Again only very exclusive analyses could allow to shed more light on the degree of equilibrium reached by the systems and on the possible role of dynamics in determining the state of the nucleus at the end of the interact-

ing phase. That is why both theoreticians and experimentalists are going back to lower energies, where multi-fragment emission is now predicted to set in and where, perhaps, it could be better characterized.

Multi-fragment emission is in fact an important decay mode, which could give information on the possible presence of a liquid-gas phase transition in nuclear matter. In this framework, statistical micro-canonical models predict, for finite isolated systems, anomalies [8] of the thermo-statistical quantities at the onset of multi-fragment production. These signals, corresponding to the opening of the phase space and to the increase of the variances of the static quantities, are expected for a first-order phase transition already at an excitation energy $\epsilon^* \approx 2.5 A$ MeV.

A back-bending of the temperature – excitation energy correlation (caloric curve $T(\epsilon^*)$ versus ϵ^* [3, 9, 10]) corresponds to the increased request of (potential) energy necessary to create IMF's and to the consequent decrease of the available thermal energy.

Another predicted signature, when a first-order phase transition occurs, is the anomalous behaviour of the heat capacity of the finite decaying system. Two divergencies in the heat capacity are expected and a negative branch between them, the distance between the poles being associated with the latent heat [11].

Thus, according to the predictions of models, the investigation of the multi-IMF decay channel, together with the study of the caloric curve and of the microcanonical heat capacity, could be a powerful tool to search for a fingerprint of a phase transitions at low-energy. These facts and the prediction of multi-fragmentation models of a non-negligible presence of the three-body emission (about 4% with respect to the probability of a binary decay) at about the energy where an S-shaped caloric curve is predicted, underline the importance of searching for a possible three- (or more) body decay at low excitation energies.

2. *Experimental set-up*

The measurements have been performed at the Tandem–ALPI accelerator of the Laboratori Nazionali di Legnaro (LNL, Padua, Italy), with the experimental apparatus designed to work at the available beam-energy range (from 6 to 20 A MeV). The apparatus is composed of a couple of newly designed complex drift chambers (the GARFIELD detector), and an annular three-stage detector at forward angles. A schematic picture of the apparatus is shown in Fig. 1.

The two GARFIELD drift chambers cover almost completely the ϕ angular range, while the θ angle goes from 30° to 85° and from 95° to 150° , respectively. Only the forward part was actually used in the present measurements and operated with CF_4 at a pressure of 70 mbar. Electrons formed along the primary ionisation tracks of the impinging particles drift toward the anodic plane where they are multiplied by 96 micro-strip gaseous detectors, giving information on the energy loss ΔE and the θ angle [12, 13]. Moreover, 96 CsI(Tl) crystals with photodiode readout were located in the same gas volume for the determination of residual

energy E [14, 15]. The GARFIELD detector can identify from light charged particles to heavy fragments with an energy threshold of about 1 A MeV.

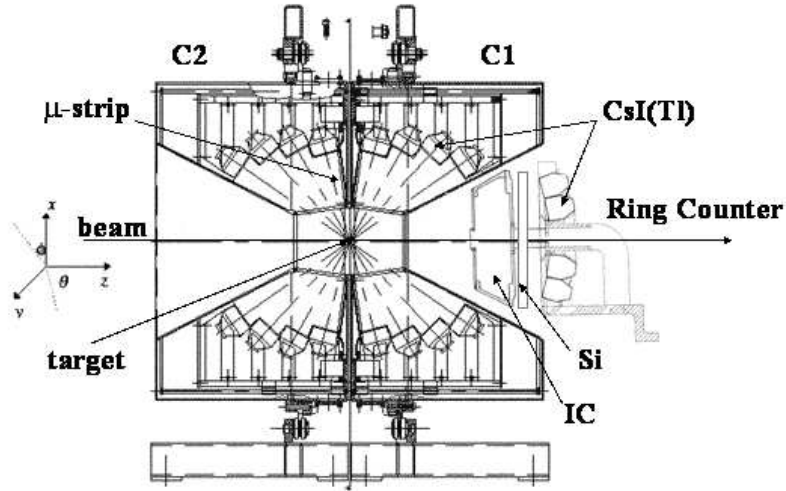


Fig. 1. Schematic drawing of the experimental apparatus: the two drift chambers (C1 and C2) are located back to back, with the target in between, while the annular detector is positioned in the forward direction with respect to the beam.

The annular detector is placed at a distance of 16 cm from the target and covers the θ angular range from 6° to 18° and almost completely the ϕ angles. It is divided into 8 sectors, each of which consisting of an axial ionization chamber, a $300\ \mu\text{m}$ thick Si strip-detector and 2 CsI(Tl) crystals with photodiode readout. Each sector of the Si detector is divided into 8 strips, giving a determination of the scattering angles within $\Delta\theta = \pm 0.7^\circ$ and $\Delta\phi = \pm 22.5^\circ$. In this case too, the energy threshold for the identification of light charged particles and fragments is about 1 A MeV.

The first measurement was performed using an 11 A MeV ^{32}S beam on $^{58,64}\text{Ni}$ targets $250\ \mu\text{g}\cdot\text{cm}^{-2}$ thick. The grazing angle for these reactions was 11° . For the considered reactions, the laboratory angles covered by GARFIELD correspond to centre-of-mass angles from 50° to 130° .

3. Results and discussion

The experimental probability distributions of light charged particles and IMFs are shown in the left and right panels of Fig. 2, respectively. The dashed lines represent the events detected by the whole apparatus, the solid lines are those detected only in the GARFIELD array.

Experimentally, the percentage of the three-IMF events with respect to the two-IMF ones is 4% and 3% for events detected by the whole apparatus and by GARFIELD, respectively. These values are in agreement with those predicted both

by the sequential statistical models like GEMINI [2] and the statistical multi-fragmentation models like SMM [3, 4] ($\sim 4\%$). This confirms what was already pointed out many times in the literature: no selective information on the reaction mechanisms can be deduced by inclusive quantities. More selective analyses are necessary to disentangle the various possibilities.

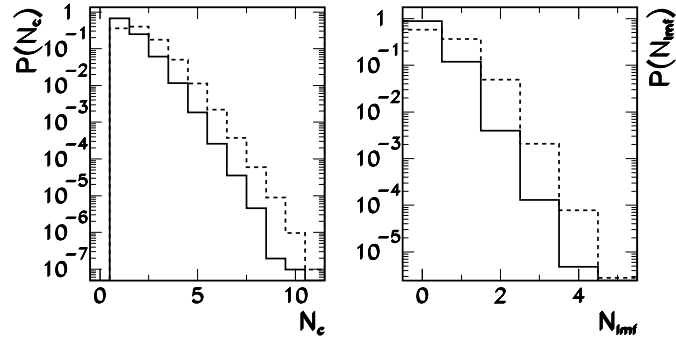


Fig. 2. $^{32}\text{S} + ^{58}\text{Ni}$ reaction at 11 A MeV. Experimental charged-particle (left) and IMF (right) multiplicity distributions. The yields are normalized to their sum. The dashed lines represent the distributions of products detected by the whole apparatus, the solid lines the distributions of those detected by GARFIELD only.

The first step in the analysis was the introduction of restrictions on the impact parameter range, selecting central collisions within the observed ones. In this direction, the class of events was extracted with no heavy fragments in the forward annular detector but at least two α -particles and three or more IMFs in GARFIELD. The requirement of high multiplicity (at least 5 charged products in this case) at large centre-of-mass angles should correspond to violent collisions. As shown in Fig. 3, in collisions where three or more fragments are detected at large centre-of-mass angles, the azimuthal α -particle correlation function shows no preferential emission angle and displays a practically isotropic correlation function, as one expects for central collisions.

An estimate of the angular momentum of the emitting system can be deduced performing a comparison with model predictions. In particular, calculations were performed with the GEMINI statistical sequential model [2] for angular momentum from 0 to $55 \hbar$, the latter value being the maximum value for which the fusion of the two reaction partners is permitted according to the Bass model [16]. Predictions for an $\langle L \rangle$ value of $48 \hbar$ show a quite strong U-shaped α -particle correlation function, peaked around $\Delta\phi = 0^\circ$ and $\Delta\phi = 180^\circ$, as expected if the emitting source of the α -particles is supposed to rotate quite rapidly. The experimental correlation function for the selected data agrees on the contrary with model calculations performed with a much lower $\langle L \rangle$ value ($10 \hbar$), corresponding for this reaction to an impact parameter $b \approx 1$ fm, which confirms the indication that those events should correspond to central collisions.

This evaluation of centrality is also supported by a comparison of other ex-

perimental quantities with the prediction of CMD [5, 6], filtered through the experimental apparatus acceptance. The distributions of events as a function of the

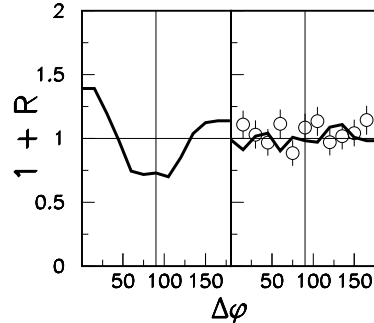


Fig. 3. $^{32}\text{S} + ^{58}\text{Ni}$ reaction at 11 A MeV. Azimuthal correlation function for α -particles detected in GARFIELD, gated by three IMFs detected at large angles in the GARFIELD drift chamber. Left panel: correlation function calculated with the sequential statistical model code GEMINI for $\langle L \rangle = 48 \text{ h}$. Right panel: experimental data and GEMINI calculation for $\langle L \rangle = 10 \text{ h}$.

impact parameter b and the centre-of-mass angle θ_{cm} clearly demonstrate that a requirement of at least three IMFs in GARFIELD only (Fig. 4, fourth upper panel) selects central impact parameters, so that the average impact parameter resulting

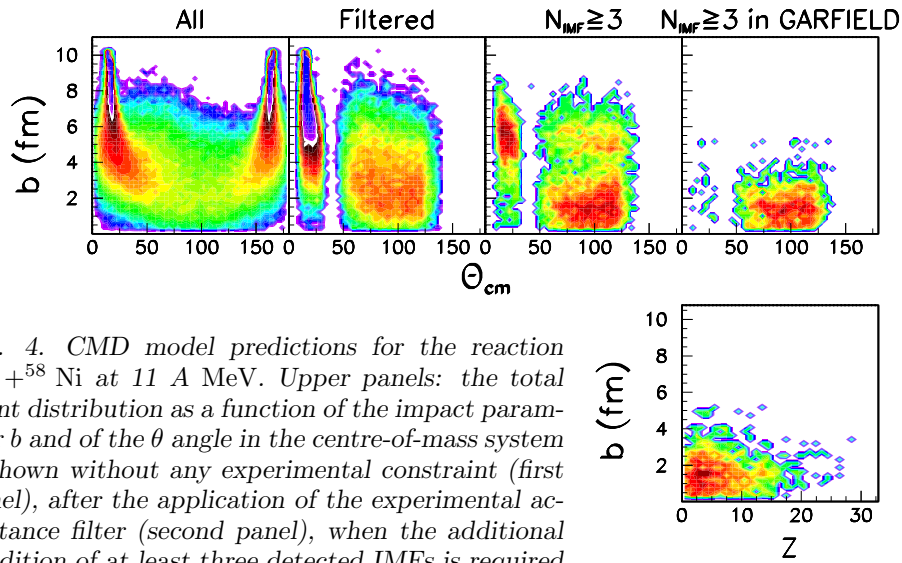


Fig. 4. CMD model predictions for the reaction $^{32}\text{S} + ^{58}\text{Ni}$ at 11 A MeV. Upper panels: the total event distribution as a function of the impact parameter b and of the θ angle in the centre-of-mass system is shown without any experimental constraint (first panel), after the application of the experimental acceptance filter (second panel), when the additional condition of at least three detected IMFs is required in the whole apparatus (third panel) or in GARFIELD only (fourth panel). Bottom panel: a scatter plot of the correlation between charge of emitted IMFs and impact parameter is shown for the (experimental) events corresponding to the fourth-upper panel.

from this selection is $\langle b \rangle \approx 2$ fm. Figures 5 and 6 show, respectively, the experimental and CMD simulated elemental distributions $N(Z)$ for events in which at least three IMFs have been detected in the whole apparatus (open symbols) and in GARFIELD only (full symbols). It is obvious that the selection with GARFIELD eliminates the elastic and quasi-elastic contribution around $Z = 16$. CMD calculations do not include this kind of outgoing channels.

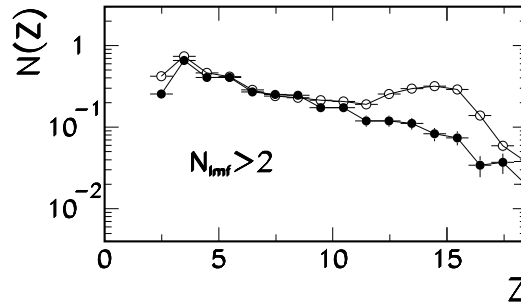


Fig. 5. $^{32}\text{S} + ^{58}\text{Ni}$ reaction at 11 A MeV. Charge distribution of IMFs detected in the whole apparatus (open symbols) and in GARFIELD (full symbols) for events with at least three IMFs. Both charge distributions are normalized to the total number of events.

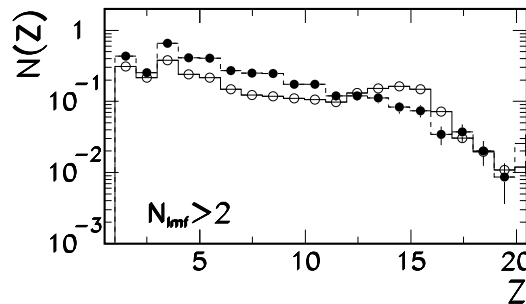


Fig. 6. $^{32}\text{S} + ^{58}\text{Ni}$ reaction at 11 A MeV. Filtered CMD charge distribution for events with at least three IMFs: open symbols refer to events detected in the whole apparatus, full symbols to events detected in GARFIELD. As shown in Fig. 4, this results in $\langle b \rangle \approx 2$ fm. Both charge distributions are normalized to the total number of events.

Let us elaborate in more detail the central events. For well detected events (total detected charge about 70% of the total charge), we show in Fig. 7 the charge partition (left panel), i.e. the elemental multiplicity distribution of the largest fragment (squares), the second largest one (full points) and the third largest fragment (circles). In a more suggestive way, the data are presented by means of the Dalitz plot [17] in the right panel of the same figure. In this picture, let Z_1, Z_2, Z_3 be

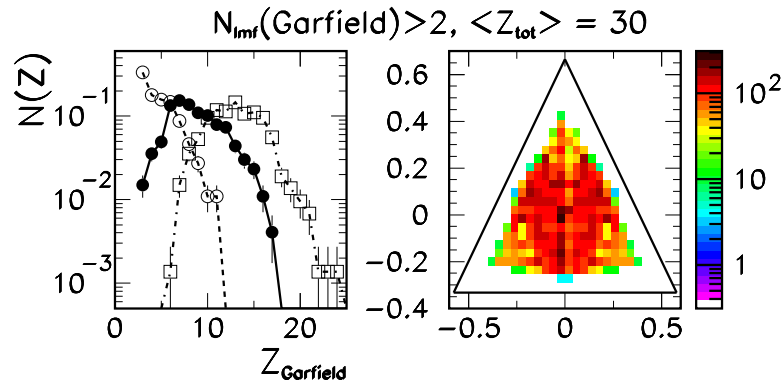


Fig. 7. $^{32}\text{S} + ^{58}\text{Ni}$ reaction at 11 A MeV. Charge distribution of the three largest IMFs detected in each event (left panel) and relative Dalitz plot for the experimental data. Both charge distributions are normalized to the total number of events.

the atomic numbers of the three considered fragments. One defines the following coordinates in a Cartesian frame: $x = (Z_2 - Z_3)/\sqrt{3}$ and $y = Z_1 - (Z_1 + Z_2 + Z_3)/3$. Then, each point of the coordinate system (x, y) lies within a triangle, the distance d_i to each side i of the triangle being equal to Z_i . Therefore, the corner of the triangle would be populated by events with one large remnant and two small fragments, the sides of the triangle are associated with fission-like events (two large fragments and a small one), while the centre is populated with equal-charge fragment events.

From Fig. 7 it appears the preponderance of events with charge symmetric splitting. This is a characteristic feature of a fast decay, as predicted by multi-fragmentation and dynamical models.

The same quantities were calculated with the dynamical CMD model [5, 6], the sequential statistical model GEMINI (with $\langle L \rangle = 48 \hbar$ in order to produce IMFs) [2] and the statistical multi-fragmentation model (SMM) [3, 4]. All the theoretical predictions were filtered for the experimental acceptance. The results are shown in Figs. 8, 9 and 10, respectively.

When dealing with the sequential statistical model predictions, the disagreement between the experimental data and the calculation is evident. In fact, if one considers an average angular momentum of $10 \hbar$, as the one derived by α -particle correlation distribution, no three IMF events are predicted by GEMINI. In any case, even considering larger ($\langle L \rangle = 48 \hbar$) angular momentum, which according to the Bass model still contributes to the fusion cross section, the sequential fragmentation of the system is very different from the experimental data. GEMINI, in fact, predicts a very asymmetric break-up, essentially made of a big fragment and two very small pieces (generally two lithium ions). The biggest one would be obviously directed in the forward part of the apparatus, so that eventually only the two small pieces could be detected in GARFIELD. GEMINI predictions are, therefore, incompatible with the experimental results, while the remaining models

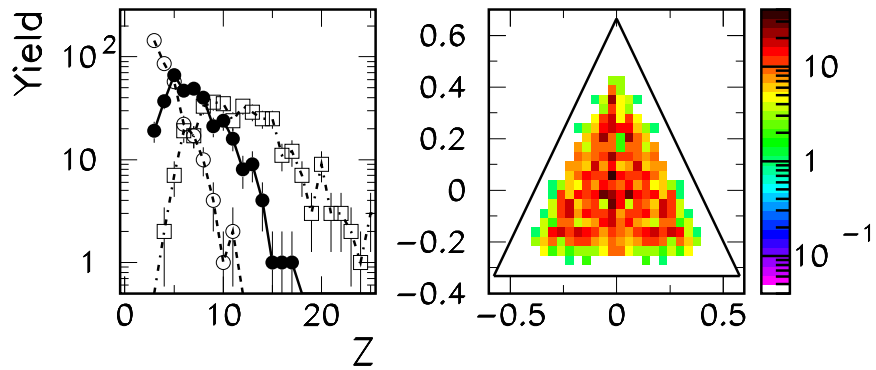


Fig. 8. Same as Fig. 7, but simulated by *CMD* dynamical model. Both charge distributions are normalized to the total number of events.

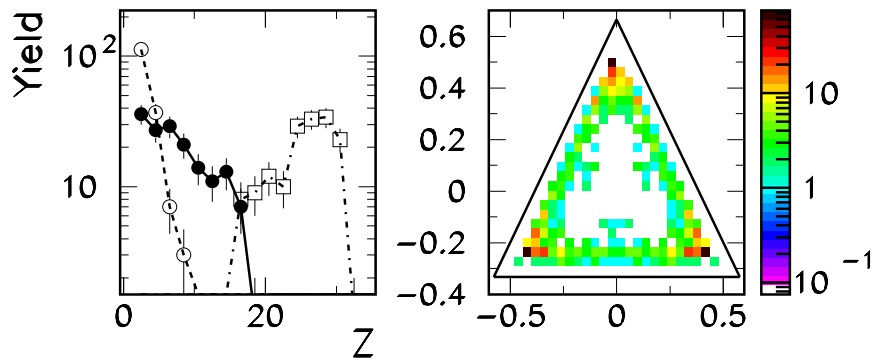


Fig. 9. Same as Fig. 7, but simulated by *GEMINI* statistical model with $\langle L \rangle = 48$ \hbar . Both charge distributions are normalized to the total number of events.

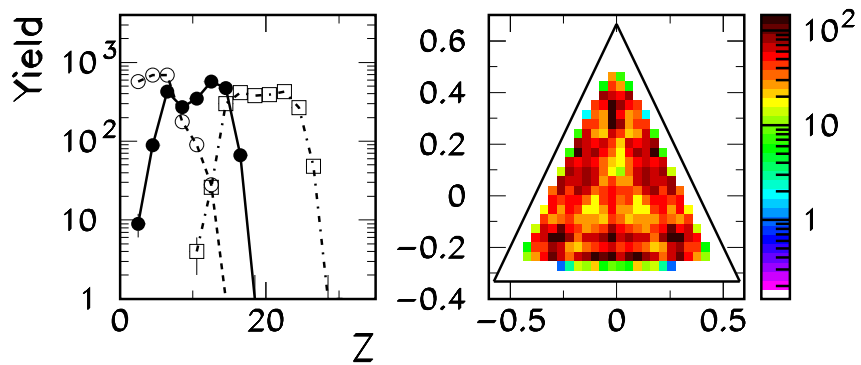


Fig. 10. Same as Fig. 7, but simulated by *SMM* statistical multi-fragmentation model. Both charge distributions are normalized to the total number of events.

seem to better describe them. Indeed, the feature of the CMD and SMM distributions, where all the three IMFs were detected by GARFIELD only, is close to the experimental conditions. In any case, before claiming that an instantaneous multi-fragmentation has been observed at such a low excitation energy, a deeper analysis has to be performed on velocity correlations among IMFs, in order to provide an estimate of their average emission time.

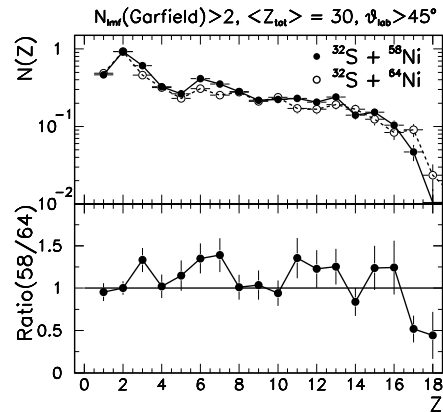


Fig. 11. Charge distribution (upper panel) in the reactions $^{32}\text{S}+^{58}\text{Ni}$ and $^{32}\text{S}+^{64}\text{Ni}$, for events with at least three IMFs detected in GARFIELD. In the lower panel, the ratio of the two charge distributions is shown. Both charge distributions are normalized to the total number of events.

Another interesting finding comes from the comparison of the charge distributions of IMFs, detected at large centre-of-mass angles, for the two reactions here considered, i.e. by changing the neutron content of the system. In fact, the charge distribution for the $^{32}\text{S}+^{58}\text{Ni}$ ($N/Z = 1.05$) and $^{32}\text{S}+^{64}\text{Ni}$ ($N/Z = 1.18$) reactions differs (Fig. 11, upper part) by values larger than the statistical errors. This effect is highlighted when the ratio of the two charge distributions is performed (Fig. 11, lower part). It would probably be more pronounced when comparing reactions where the N/Z values of the compound system differ by larger amounts and could be ascribed to the opening/closure of the decay channels, due to the energy conservation constraint on the phase space. However, the statistics collected for these targets is not sufficient to draw any definite conclusion, and at these energies other effects, like for example the effects of nuclear structure, could be still very strong. Moreover, a very good selection of the emitting source should be performed in order to do meaningful comparisons. Therefore, more refined data are necessary to investigate this interesting observation.

4. Conclusions

The $^{32}\text{S}+^{58,64}\text{Ni}$ reaction at 11 A MeV was studied at the Tandem-ALPI facility of the LNL to search for a possible onset of multi-fragmentation processes

at low energy. This was incited by the renewed interest for the low-medium energy range, where multifragmentation processes could start in a more clear and distinguishable way, thus bringing more detailed information on the reaction mechanisms. Moreover, theoretical predictions indicate in this energy range the region where the opening of new channels in the phase space could evidence a signature for a phase transition of nuclear matter.

Both α - α experimental correlation functions, tagged by highly charged IMF multiplicity detected at large angles, and the comparison with theoretical dynamical calculations, give indication on the presence of central events, for which the composite system breaks down in many IMFs. The charge distributions of the three largest IMFs relative to “well detected events” indicate that events with three final IMFs of similar charge are strongly favoured, which is a major indication of the instantaneous break-up of the system. By comparing the charge distribution of IMFs detected at large centre-of-mass angles, evidence for a different production of IMFs as a function of the neutron content of the system has been found. The question whether this is due to the isospin effects or to the structure effects will be further studied in future experiments at larger statistics.

Acknowledgements

The authors are indebted to A. Boiano, R. Cavaletti, A. Cortesi, P. Del Carmine, M. Giacchini and G. Tobia for their skillful assistance. This work was supported in part by grants of the Italian Ministry of Instruction, University and Research (MIUR) and of Alma Mater Studiorum of the Bologna University.

References

- [1] S. J. Sanders, A. Szanto de Toledo and C. Beck, *Phys. Rep.* **311** (1999) 487.
- [2] R. J. Charity, M. A. McMahan, G. J. Wozniak, R. J. McDonald, L. G. Moretto, D. G. Sarantites, L. G. Sobotka, G. Guarino, A. Pantaleo, L. Fiore, A. Gobbi and K. D. Hildenbrand, *Nucl. Phys. A* **483** (1988) 371.
- [3] D. H. E. Gross, *Rep. Prog. Phys.* **53** (1990) 605; *Phys. Rep.* **279** (1997) 119.
- [4] J. P. Bondorf, A. S. Botvina, A. S. Iljinov, I. N. Mishustin and K. Sneppen, *Phys. Rep.* **257** (1995) 133.
- [5] M. Belkacem, V. Latora and A. Bonasera, *Phys. Rev. C* **52** (1995) 271.
- [6] A. Bonasera, M. Bruno, C. O. Dorso and P. F. Mastinu, *Riv. Nuovo Cimento* **23**, no. 2 (2000) 1.
- [7] R. Nebauer and J. Aichelin, *Nucl. Phys. A* **650** (1999) 65.
- [8] Ph. Chomaz and F. Gulminelli, *Nucl. Phys. A* **647** (1999) 153.
- [9] D. H. E. Gross, M. E. Madjet and O. Schapiro, *Z. Phys. D* **39** (1997) 75.
- [10] A. Le Fèvre, O. Schapiro and A. Chbihi, *Nucl. Phys. A* **657** (1999) 446.
- [11] M. D’Agostino, F. Gulminelli, Ph. Chomaz, M. Bruno, F. Cannata, R. Bougault, F. Gramagna, I. Iori, N. Le Neindre, G. V. Margagliotti, A. Moroni and G. Vannini, *Phys. Lett. B* **473** (2000) 219.

- [12] F. Gramegna, U. Abbondanno, A. Andreano, R. Bassini, F. Bonutti, M. Bruno, G. Casini, M. D'Agostino, G. Manzin, G. V. Margagliotti, P. F. Mastinu, P. M. Milazzo, A. Moroni, M. Squarcini, F. Tonetto, G. Vannini and L. Vannucci, Nucl. Instr. Meth. A **389** (1997) 474.
- [13] M. Chiari, A. Lanchais, F. Tonetto and L. Travaglini, Nucl. Instr. Meth. A **484** (2002) 111.
- [14] F. Tonetto, U. Abbondanno, M. Chiari, P. M. Milazzo and L. Travaglini, Nucl. Instr. Meth. A **420** (1999) 181.
- [15] U. Abbondanno, M. Bruno, G. Casini, R. Cavaletti, Sl. Cavallaro, M. Chiari, M. D'Agostino, F. Gramegna, A. Lanchais, G. V. Margagliotti, P. F. Mastinu, P. M. Milazzo, A. Moroni, A. Nannini, A. Ordine, G. Vannini and L. Vannucci, Nucl. Instr. Meth. A **488** (2002) 604.
- [16] R. Bass, *Nuclear Reactions with Heavy Ions*, Springer Verlag, Berlin (1980).
- [17] P. Kreutz, J. C. Adloff, M. Begemann-Blaich, P. Bouissou, J. Hubele, G. Immè, I. Iori, G. J. Kunde, S. Leray, V. Lindenstruth, Z. Liu, U. Lynen, R. J. Meijer, U. Milkau, A. Moroni, W. F. J. Müller, C. Ngô, C. A. Ogilvie, J. Pochodzalla, G. Raciti, G. Rudolf, H. Sann, A. Schüttauf, W. Seidel, L. Stuttge, W. Trautmann and A. Tucholski, Nucl. Phys. A **556** (1993) 672.

VIŠE-FRAGMENTNA TVORBA U REAKCIJAMA $^{32}\text{S}+^{58,64}\text{Ni}$ NA 11 A MeV

Istraživali smo značajke reakcije $^{32}\text{S}+^{58,64}\text{Ni}$ na 11 A MeV radi pronalaženja mogućeg porasta više-fragmentnih procesa na nižim uzbudnim energijama. Važnost se tih pojava sastoji u tome što bi one mogle predstavljati znakove nuklearnog faznog prijelaza od tekućeg u plinsko stanje. Znakovi tvorbe više fragmenata vide se u dobivenim podacima; no čak ako je i prinos tih događaja u skladu s predviđanjima statističkog modela, razdioba mase sustava koji se raspada ne uspijeva se objasniti. Usporedba dviju reakcija ukazuje na moguće izospinske efekte.